are required to elucidate whether the frequencies of heterozygous mutation carriers in ISS differ, depending on ethnicities.

R110C showed defective trafficking from the ER to the Golgi apparatus. Subcellular localization studies have shown that 11 of 12 missense *NPR2* mutations, which were identified in AMDM patients, caused ER retention (15). Therefore, defective cellular trafficking from the ER to the plasma membrane is likely a major molecular mechanism of the missense *NPR2* mutations. Protein folding in the ER is monitored by ER quality control mechanisms, and misfolding proteins are retained and degraded in the ER by an ER-associated degradation pathway (16). We speculate that a change in conformation of the mutant NPR-B receptor promotes protein misfolding and defects in the normal intracellular trafficking from the ER to the Golgi apparatus.

In contrast to R110C, Q417E was expressed normally on the plasma membrane. We hypothesize that the pathogenesis of Q417E may be defective in ligand binding or receptor activation. Particularly, Gln417 is located in the junctional region between the ligand binding domain and the transmembrane domain. According to an investigation using an NPR-A crystal structure, counterclockwise rotation of juxtamembrane regions of a dimer is prerequisite for initiating transmembrane signaling by ligand binding (17). This rotation, which is transduced across the membrane, can reorient the intracellular domains and activate guanylyl cyclase. If the rotation of the NPR-A receptor is applied to the NPR-B receptor, a juxtamembrane region of NPR-B, including Gln417 might also play a critical role in initializing transmembrane signaling.

R110C and Q417E showed dominant-negative effects on the coexpressed WT receptor. Previously, four missense mutations (S76P, R263P, L658F, and R819C) were demonstrated to have dominant-negative effects (8, 13), but molecular mechanisms have not been elucidated. Our coexpression experiments indicated that R110C, which has defective trafficking from the ER to the Golgi apparatus, interacted with WT-NPR-B and relatively reduced the abundance of a fully glycosylated receptor. Some receptor mutants (eg, GnRH receptor, melanocortin 1 receptor, and $\alpha$2-adrenergic receptor) were reported to have dominant-negative effects by heterodimerizing with and entrapping the WT receptor in the ER (18–20). A similar pathological mechanism can be true for the dominant-negative effect of R110C. Our coexpression experiments also showed that Q417E expressing on the plasma membrane interacted with WT-NPR-B. Q417E probably functions as a dominant-negative mutant, suppressing the activation and response of WT-NPR-B by forming an unproductive heterodimer, WT-NPR-B/Q417E.

In contrast, the I364fs mutant lacking the transmembrane domain was not thought to have a dominant-negative effect (ie, haploinsufficiency) (12). These findings necessitate the reinvestigation of other heterozygous *NPR2* mutations to discriminate whether the pathological effects (a dominant negative effect or haploinsufficiency) on WT-NPR-B in vitro significantly influence clinical phenotypes.

We provided observational data that were consistent with the hypothesis that a monoallelic *NPR2* mutation could cause short stature. However, we have not rigorously verified that hypothesis. It would be of interest to have genotype and phenotype information for the extra family member, as reported in the paper by Olney (12).

In summary, we identified two heterozygous loss-of-function *NPR2* mutations in a Japanese cohort with short stature. Both mutations had a dominant-negative effect, and their dominant-negative mechanisms varied corresponding to the molecular pathogenesis of *NPR2* mutations. Further studies involving other mutants should be conducted to clarify the pathological roles of different mutations in long bone growth.

## Acknowledgments

We acknowledge the resources provided by the Japan Growth Genome Consortium. We also acknowledge Dr Rumi Hachiya and Professor Yoshihiro Ogawa for kindly providing HA-WT-NPR-B construct, Professor Takao Takahashi for fruitful discussion, and Professor Kenji Fujieda for supporting this study. Kenji Fujieda died at March 19, 2010.

Address all correspondence and requests for reprints to: Tomonobu Hasegawa, MD, PhD, Department of Pediatrics, Keio University School of Medicine, Shinanomachi 35, Shinjuku-ku, Tokyo 160–8582, Japan. E-mail: thaseg@a6.keio.jp.

This work was supported by Novo Nordisk and the Health Science Research Grant for Research on Applying Health Technology [Jitsuyoka (Nanbyo)-Ippan-014] from the Ministry of Health, Labor, and Welfare, Japan.

Disclosure Summary: The authors have nothing to disclose.

## References

1. **Pejchalova K, Krejci P, Wilcox WR.** C-natriuretic peptide: an important regulator of cartilage. *Mol Genet Metab.* 2007;92:210–215.
2. **Olney RC.** C-type natriuretic peptide in growth: a new paradigm. *Growth Horm IGF Res.* 2006;16(suppl A):S6–S14.
3. **Yasoda A, Nakao K.** Translational research of C-type natriuretic peptide (CNP) into skeletal dysplasias. *Endocr J.* 2010;57:659–666.
4. **Komatsu Y, Chusho H, Tamura N, et al.** Significance of C-type natriuretic peptide (CNP) in endochondral ossification: analysis of CNP knockout mice. *J Bone Miner Metab.* 2002;20:331–336.
5. **Sogawa C, Tsuji T, Shinkai Y, Katayama K, Kunieda T.** Short-

limbed dwarfism: slw is a new allele of Npr2 causing chondrodysplasia. *J Hered.* 2007;98:575–580.
6. **Banapurmath CR, Patil M, Guruprasad G, Kesaree N.** Acromesomelic dysplasia of the Maroteaux type. *Indian J Pediatr.* 1990; 57:803–805.
7. **Bartels CF, Bukulmez H, Padayatti P, et al.** Mutations in the transmembrane natriuretic peptide receptor NPR-B impair skeletal growth and cause acromesomelic dysplasia, type Maroteaux. *Am J Hum Genet.* 2004;75:27–34.
8. **Hachiya R, Ohashi Y, Kamei Y, et al.** Intact kinase homology domain of natriuretic peptide receptor-B is essential for skeletal development. *J Clin Endocrinol Metab.* 2007;92:4009–4014.
9. **Khan S, Ali RH, Abbasi S, Nawaz M, Muhammad N, Ahmad W.** Novel mutations in natriuretic peptide receptor-2 gene underlie acromesomelic dysplasia, type maroteaux. *BMC Med Genet.* 2012; 13:44.
10. **Miura K, Namba N, Fujiwara M, et al.** An overgrowth disorder associated with excessive production of cGMP due to a gain-of-function mutation of the natriuretic peptide receptor 2 gene. *PloS One.* 2012;7:e42180.
11. **Hannema SE, van Duyvenvoorde HA, Premsler T, et al.** 2013 An activating mutation in the kinase homology domain of the natriuretic peptide receptor-2 causes extremely tall stature without skeletal deformities. *J Clin Endocrinol Metab.* 2013;98(12):E1988–E1998.
12. **Olney RC, Bukulmez H, Bartels CF, et al.** Heterozygous mutations in natriuretic peptide receptor-B (NPR2) are associated with short stature. *J Clin Endocrinol Metab.* 2006;91:1229–1232.
13. **Gabriela GA, Amano N, Docko AJ, et al.** Heterozygous mutations in natriuretic peptide receptor-B gene (NPR2) as a cause of idiopathic short stature. *J Clin Endocrinol Metab.* 2013;98:E1636–E1644.
14. **Inoue H, Kangawa N, Kinouchi A, et al.** Identification and functional analysis of novel human growth hormone secretagogue receptor (GHSR) gene mutations in Japanese subjects with short stature. *J Clin Endocrinol Metab.* 2011;96:E373–E378.
15. **Hume AN, Buttgereit J, Al-Awadhi AM, et al.** Defective cellular trafficking of missense NPR-B mutants is the major mechanism underlying acromesomelic dysplasia-type Maroteaux. *Hum Mol Genet.* 2009;18:267–277.
16. **Vembar SS, Brodsky JL.** One step at a time: endoplasmic reticulum-associated degradation. *Nat Rev Mol Cell Biol.* 2008;9:944–957.
17. **Ogawa H, Qiu Y, Ogata CM, Misono KS.** Crystal structure of hormone-bound atrial natriuretic peptide receptor extracellular domain: rotation mechanism for transmembrane signal transduction. *J Biol Chem.* 2004;279:28625–28631.
18. **Brothers SP, Cornea A, Janovick JA, Conn PM.** Human loss-of-function gonadotropin-releasing hormone receptor mutants retain wild-type receptors in the endoplasmic reticulum: molecular basis of the dominant-negative effect. *Mol Endocrinol (Baltimore, MD).* 2004;18:1787–1797.
19. **Sanchez-Laorden BL, Sanchez-Mas J, Martinez-Alonso E, Martinez-Menarguez JA, Garcia-Borron JC, Jimenez-Cervantes C.** Dimerization of the human melanocortin 1 receptor: functional consequences and dominant-negative effects. *J Invest Dermatol.* 2006; 126:172–181.
20. **Zhou F, Filipeanu CM, Duvernay MT, Wu G.** Cell-surface targeting of $\alpha$2-adrenergic receptors—inhibition by a transport deficient mutant through dimerization. *Cell Signal.* 2006;18:318–327.

Novel Insights from Clinical Practice

HORMONE RESEARCH IN PÆDIATRICS

Horm Res Paediatr 2014;81:133–138
DOI: 10.1159/000355279

Received: April 24, 2013
Accepted: August 21, 2013
Published online: January 18, 2014

# A Novel Mutation in SOX2 Causes Hypogonadotropic Hypogonadism with Mild Ocular Malformation

Masaki Takagi [a, b] Satoshi Narumi [a] Yumi Asakura [c] Koji Muroya [c]
Yukihiro Hasegawa [b] Masanori Adachi [c] Tomonobu Hasegawa [a]

[a]Department of Pediatrics, Keio University School of Medicine Tokyo, and [b]Department of Endocrinology and Metabolism, Tokyo Metropolitan Children's Medical Center, Tokyo, and [c]Department of Endocrinology and Metabolism, Kanagawa Children's Medical Center, Yokohama, Japan

**Established Facts**

- Heterozygous *SOX2* mutations have been reported to cause isolated hypogonadotropic hypogonadism (HH) in addition to ocular and brain abnormalities.
- The most common ocular phenotype associated with *SOX2* mutations is a severe bilateral eye defect such as anophthalmia or severe microphthalmia.

**Novel Insights**

- We report a novel missense *SOX2* (Y110C) mutation in an HH patient with mild ocular malformation, unilateral retinal detachment.
- The findings in this patient emphasize the importance of testing for *SOX2* mutations in HH individuals with mild ocular defects, such as retinal detachment, in the absence of anophthalmia or severe microphthalmia.
- We used a next-generation sequencing strategy to analyze 122 genes associated with congenital endocrine disorders. This approach is new in HH; it has never been reported to our knowledge.

**Key Words**
SOX2 · Hypogonadotropic hypogonadism · HMG domain · Targeted next-generation sequencing

**Abstract**
***Background:*** Heterozygous *SOX2* mutations have been reported to cause isolated hypogonadotropic hypogonadism (HH) in addition to ocular and brain abnormalities. ***Objective:*** We report a novel missense *SOX2* (Y110C) mutation in an HH patient with mild ocular malformation. ***Patients:*** The 20-year-old male was referred because of typical signs of complete hypogonadism, with small intrascrotal testes (2 ml), no pubic hair (P1), and a micropenis. Hormone assays revealed very low plasma testosterone levels and very low levels of plasma gonadotropin. He was found to have retinal detachment in his right eye and surgery was performed at the age of 14 years. ***Results:*** Using a next-generation se-

KARGER

E-Mail karger@karger.com
www.karger.com/hrp


1663–2818/14/0812–0133$39.50/0

Tomonobu Hasegawa, MD, PhD
Department of Pediatrics
Keio University School of Medicine, 35 Shinanomachi
Shinjuku-ku, Tokyo 160-8582 (Japan)
E-Mail thaseg@a6.keio.jp

quencing strategy, we identified a novel heterozygous *SOX2* mutation, c.329A>G (p.Y110C). Y110C SOX2 had reduced transactivation and no dominant negative effect. Subcellular localization revealed no significant difference between wild-type and mutant SOX2. EMSA experiments showed that the Y110C SOX2 abrogated DNA-binding ability. ***Conclusion:*** The Y110C mutation affects a critical residue in the SOX2 protein. This study extends our understanding of the phenotypic features, molecular mechanism, and developmental course associated with mutations in *SOX2*. When multiple genes need to be analyzed for mutations simultaneously, targeted sequence analysis of interesting genomic regions is an attractive approach. 

## Introduction

Hypogonadotropic hypogonadism (HH) is a genetically heterogeneous condition, defined by absent or incomplete sexual maturation secondary to gonadotropin deficiency. Several genes have been linked to the pathogenesis of HH, including *KAL1*, *FGFR1*, *FGF8*, *PROK2*, *PROKR2*, *CHD7*, *GNRHR*, *GNRH1*, *KISS1R*, *KISS1*, *TAC3*, *TACR3*, and *SOX2* [1–8].

Heterozygous mutations in *SOX2* were first reported in patients with bilateral anophthalmia or severe microphthalmia who had additional abnormalities, including developmental delays, learning difficulties, esophageal atresia, and genital abnormalities [9–11]. Subsequently, *SOX2* mutations were also shown to be associated with anterior pituitary hypoplasia, HH, and variable growth hormone deficiency in association with other manifestations, including hippocampal abnormalities, defects of the corpus callosum, hypothalamic hamartoma, and sensorineural hearing loss [7, 8]. To date, more than 40 mutations in *SOX2* have been described [12]. The majority of these are truncating mutations such as nonsense or frameshift mutations, and only 10 missense mutations have been reported.

Here, we report an HH patient with mild ocular phenotypes carrying a novel missense mutation in *SOX2* (Y110C). Through molecular analyses, we showed that substitution of a conserved, critical amino acid near the DNA-binding high-mobility group (HMG) domain of SOX2 abrogated DNA-binding and pituitary gene *(HESX1)* activation. This study extends our understanding of the phenotypic features, molecular mechanism, and developmental course associated with mutations in the *SOX2* gene.

**Table 1.** Endocrinological findings (baseline) in the propositus

| | 20 years | Reference (adult) |
|---|---|---|
| IGF-1, ng/ml | 307 | male: 41–369 |
| TSH, μU/ml | 2.42 | 0.3–3.50 |
| Free T4, ng/dl | 1.15 | 1.09–2.55 |
| Free T3, pg/ml | 3.82 | 3.23–5.11 |
| LH, mIU/ml | 0.1 | male: 2.2–8.4 |
| FSH, mIU/ml | 0.31 | male: 1.8–12 |
| Testosterone, ng/ml | 0.38 | male: 2.01–7.50 |

The conversion factors to the SI units are as follows: IGF-I 0.131 (nmol/l), TSH 1.0 (mIU/l), free T4 12.87 (pmol/l), free T3 1.54 (pmol/l), LH 1.0 (IU/l), FSH 1.0 (IU/l), and testosterone 0.035 (nmol/l).

## Materials and Methods

*Case Report*

The propositus was a 23-year-old Japanese man born at 41 weeks of gestation after an uncomplicated pregnancy and delivery. The parents were nonconsanguineous and phenotypically normal. He had one younger sister who had no relevant clinical problems. His birth weight was 3,250 g (+0.6 SD), and length was 49.0 cm (0.0 SD). He had horizontal nystagmus and bilateral cryptorchidism, which were diagnosed in the first months of life. No anophthalmia or microphthalmia was recorded. His gross motor development was almost normal. At the age of 3 years, he presented with generalized seizures, which have been well controlled with sodium valproate. At the age of 14 years, he was found to have retinal detachment in his right eye and surgery was performed.

He was referred at the age of 20 years due to the typical signs of complete hypogonadism, with small intrascrotal testes (2 ml), no pubic hair (P1), and a micropenis. Hormone assays revealed very low plasma levels of testosterone and gonadotropin (table 1). Brain MRI showed a normal pituitary and olfactory bulb and no other abnormalities. He had a normal sense of smell. His karyotype was 46,XY. His height and weight were 174.4 cm (+0.7 SD) and 63.9 kg (+0.2 SD), respectively. The visual acuity of both his right and left eyes was 0.01 without glasses and 0.6 with glasses.

*Mutation Screening*

After obtaining informed consent, and with the approval of the Institutional Review Board of Keio University School of Medicine, genomic DNA was extracted from peripheral blood leucocytes of the propositus and his parents. We sequenced 13 genes implicated in HH, including *CHD7*, *FGFR1*, *FGF8*, *GNRH1*, *GNRHR*, *KAL1*, *KISS1*, *KISS1R*, *PROK2*, *PROKR2*, *TAC3*, *TACR3*, and *SOX2* using the MiSeq instrument (Illumina Inc., San Diego, Calif., USA) according to the SureSelect protocol (Agilent Technologies, Santa Clara, Calif., USA). In brief, 3 μg of genomic DNA were used for the SureSelect capture methods. Exons of 122 genes known to be associated with congenital endocrine disorders (including 13 HH-related genes) were identified in the University of California Santa

Cruz table browser (http://genome.ucsc.edu/). In total, we targeted 1,321 regions comprising 246,158 bp using SureSelect. DNA obtained from the SureSelect solution-based sequence capture was subjected to MiSeq sequencing according to the manufacturer's protocol. Base calling, read filtering, and demultiplexing were performed with the standard Illumina processing pipeline. We used BWA 0.6.1 and SAMtools 0.1.18 for alignment and variant detection against the human reference genome (NCBI build 37; hg19) with the default settings. Local realignment, quality score recalibration and variant calling were performed by GATK 2.3.9 with the default settings. We used ANNOVAR for annotation of called variants.

*Crystal Structure Modeling*

The crystal structure of the SOX2 HMG domain (protein data bank ID 1GT0; http://www.rcsb.org/pdb/) was used as a reference wild-type (WT) structure for modeling the structure of Y110C SOX2 using the PyMOL Molecular Graphics System (http://www.pymol.org).

*Functional Studies*

To generate SOX2 expression vectors, *SOX2* cDNA was cloned into pCMV-myc (Clontech, Palo Alto, Calif., USA). For subcellular localization analyses, we purchased a Halo-tagged clone vector (Kazusa DNA Research Institute, Chiba, Japan) containing human SOX2 cDNA. We introduced the Y110C mutation by site-directed mutagenesis using the PrimeSTAR Mutagenesis Basal Kit (TaKaRa, Otsu, Japan). A luciferase reporter vector was constructed by inserting the *HESX1* promoter sequence (–405 to +267 bp) into a pGL4.24 [luc2P/minP] vector (Promega, Madison, Wisc., USA). A transactivation assay was performed in HeLa cells using a dual-luciferase reporter assay system (Promega). For subcellular localization analyses, we visualized HeLa cells transfected with Halo-tagged SOX2 and TMRDirect™ ligands (Promega), according to the manufacturer's instructions. We photographed the cells using a Leica TCS-SP5 laser scanning confocal microscope (Leica, Exton, Pa., USA). The sequences of the biotin-labeled double-stranded oligonucleotide used as probe in the EMSA experiment was 5′-CAAACAAATAAACAATTAACTC -3′ [13]. Five micrograms of nuclear protein extraction was incubated at room temperature in a 20-μl binding reaction mixture containing a 20-fmol probe, 50 mM KCl, 5 mM $MgCl_2$, 2.5% glycerol, 0.05% NP-40, and 1 μg poly(dI-dC) for 20 min. For competition experiments, a large excess (200×) of unlabeled competitor oligonucleotides was included in the binding reactions. The protein-DNA complexes were subject to gel electrophoresis and transferred to a nylon membrane. The biotin-labeled probe was detected with the Lightshift Chemiluminescent EMSA Kit (Pierce).

## Results

*Mutation Screening*

We identified a novel heterozygous *SOX2* mutation, c.329A>G (p.Y110C), the only gene among 13 HH-related genes where unknown variants were identified. We used Sanger sequencing of PCR products from genomic DNA to confirm the *SOX2* variant (fig. 1a). Y110 is immediately N-terminal to the DNA-binding HMG domain, which is highly conserved among SOX proteins and is critical for binding to both interacting proteins and target DNA sequences. Y110 is a highly evolutionarily conserved amino acid (fig. 1b), and this mutation was not detected in 150 healthy Japanese controls. No sequence variation was found in *CHD7*, *FGFR1*, *FGF8*, *GNRH1*, *GNRHR*, *KAL1*, *KISS1*, *KISS1R*, *PROK2*, *PROKR2*, *TAC3*, and *TACR3*. Parental analysis was refused.

*Crystal Structural Modeling*

Y110C SOX2 was predicted to lose a residue-DNA contact (fig. 1c).

*Functional Studies*

In Hella cells, WT SOX2 stimulated transcription of the *HESX1* reporter in a dose-dependent manner. Y110C SOX2 had reduced transactivation, and had no dominant negative effect (fig. 2a). Subcellular localization revealed no significant difference between WT and mutant SOX2 (fig. 2b), indicating that nuclear targeting was not affected by the mutation. WT SOX2 specifically bound to the DNA and this binding was competed by an excess (200×) of cold competitors. In contrast, Y110C SOX2 had abrogated DNA-binding ability (fig. 2c).

## Discussion

We characterized a novel mutant (Y110C) of the SOX2 transcription factor that is associated with HH and a mild ocular phenotype. The Y110C SOX2 protein had abrogated DNA-binding affinity and decreased transcription activity compared to WT SOX2 with no dominant negative effect. The partial transcription activity suggests that the Y110C mutation is a hypomorphic mutation that retains residual activity. The most common ocular phenotype associated with *SOX2* mutations is a severe bilateral eye defect such as anophthalmia or severe microphthalmia. If an eye is present, it may be associated with ocular features, including sclerocornea. Our patient showed only unilateral retinal detachment. This mild phenotype was likely due to residual SOX2 activity. The findings in this patient emphasize the importance of testing for *SOX2* mutations in HH individuals with mild ocular defects, such as retinal detachment, in the absence of anophthalmia or severe microphthalmia.

To date, more than 40 mutations in *SOX2* have been described. Most of the mutations cause premature termination codons as a result of nonsense or frameshift muta-

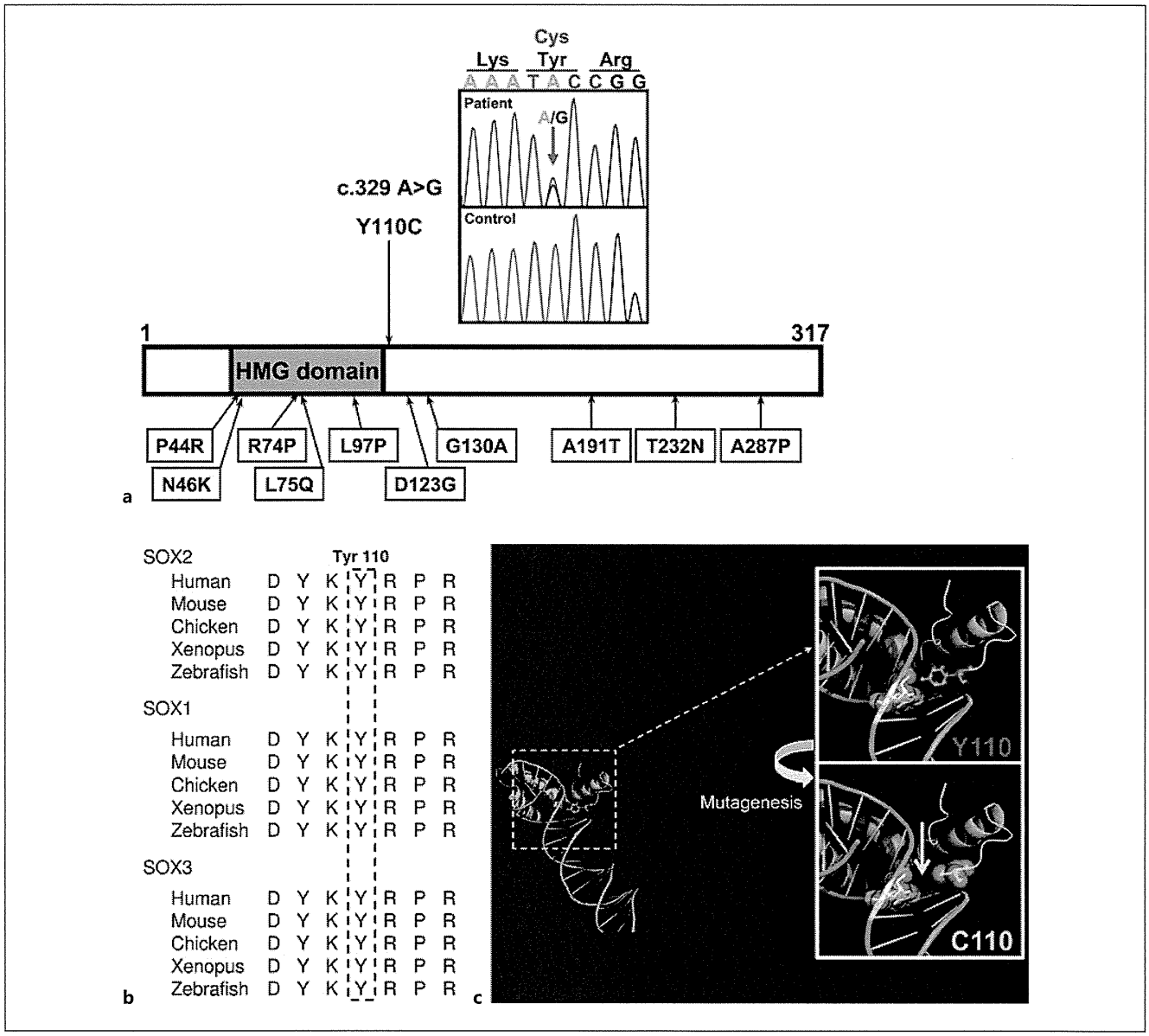


**Fig. 1.** Identification of sequence variation of *SOX2*. **a** Partial sequence of PCR product and schematic diagrams of the SOX2 protein. The chromatogram represents a heterozygous substitution of cysteine (TGC) in place of tyrosine (TAC) at codon 110. The arrow indicates the mutated nucleotide. Tyrosine 110 is located immediately 3′ of the HMG domain. The reported 10 missense mutations are summarized. **b** Homology study showed tyrosine at codon 110 is highly conserved through species in SOX2, SOX1, and SOX3. **c** Modeled structure of the Y110C in comparison with the WT structure (upper panels). Modeling of the mutant was performed using a built-in mutagenesis function of the PyMOL Molecular Graphics System. Crystal structural modeling showed Y110C SOX2 was predicted to lose a residue-DNA contact (yellow arrow).

tions; only 10 missense mutations have been reported. Among these 10 missense mutations, only 3 (R74P, L75Q, and L97P) have been confirmed as pathogenetic by functional assays [7, 10, 14]. All 3 mutations are located in the HMG domain and cause anophthalmia or severe microphthalmia. Therefore, Y110C is the only amino acid change located outside of the HMG domain that has been shown to be pathogenetic in functional assays.

Recently, Mihelec et al. [15] reported a 4-generation family with marked ocular phenotypic variability harbor-



Horm Res Paediatr 2014;81:133–138
DOI: 10.1159/000355279

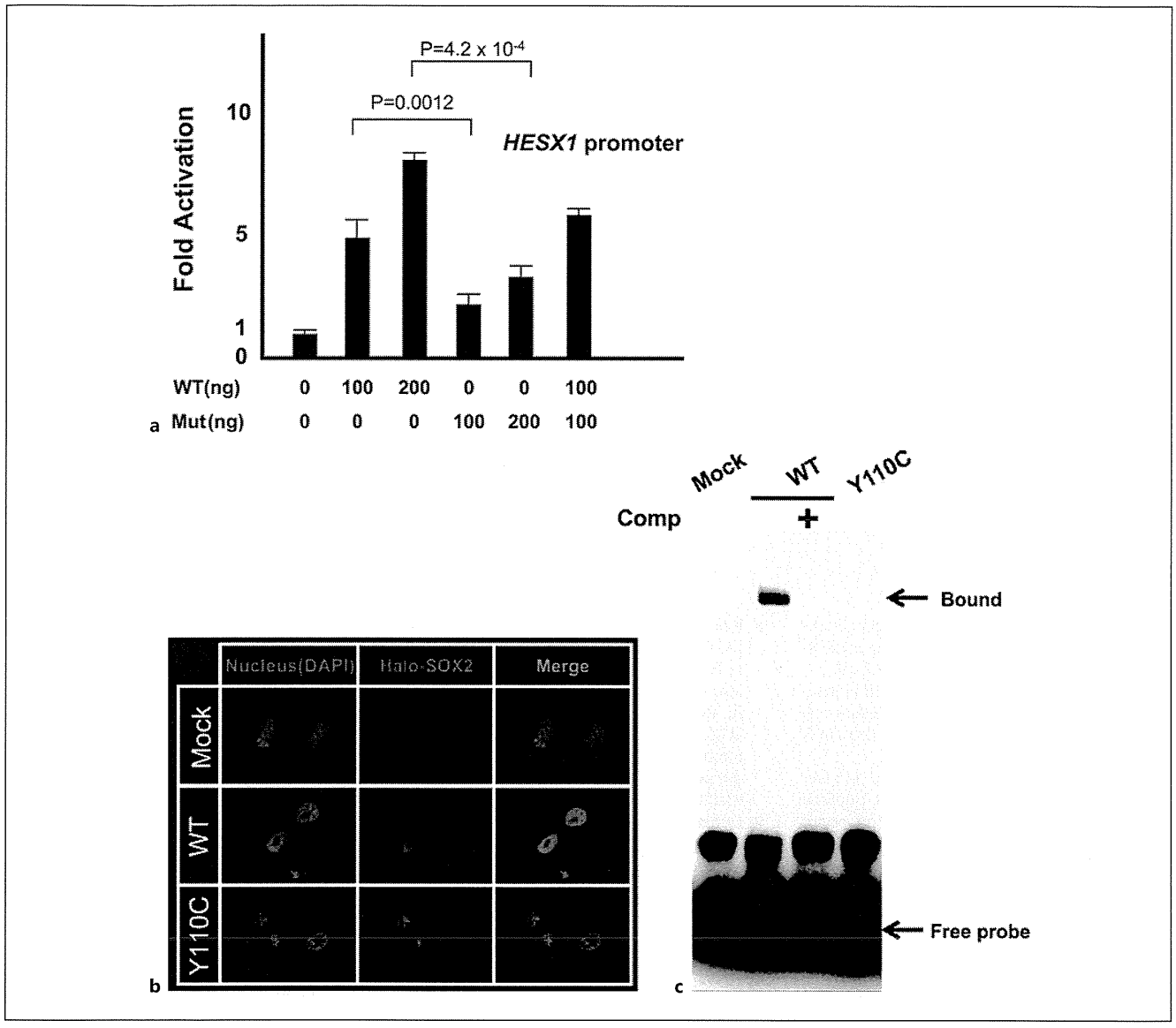


Color version available online

**Fig. 2.** Functional characterization of Y110C SOX2. **a** Transactivation assays of Y110C SOX2 using *HESX1* reporter Hela cells were cotransfected with the pRL-CMV internal control vector, indicated amount (nanograms) of the effector plasmids, and the *HESX1* reporter. WT SOX2 stimulated transcription of the *HESX1* reporter in a dose-dependent manner. Y110C SOX2 exhibited reduced transactivation and had no dominant negative effect. The data are given as means ± SEM of at least 3 independent experiments performed in triplicate transfections. **b** Subcellular localization analysis. For subcellular localization analyses, we visualized and photographed Hela cells transfected with Halo-tagged SOX2 using a Leica TCS-SP5 laser scanning confocal microscope, after mounting the cells in a Vectashield-DAPI solution. The WT and Y110C SOX2 are localized to the nucleus. **c** EMSA experiments. WT SOX2 showed specific binding to the elements, which was competed by an excess amount of (200×) cold competitors. The Y110C SOX2 showed abrogated DNA-binding ability.

ing a D123G SOX2 mutation. These multigenerational patients suggested that there had been no fertility problems in the carriers of the D123G SOX2 mutation. D123G is located immediately C-terminal to the HMG domain, which was described as a partner-factor interaction region by Mihelec et al. [15]. SOX transcription factors exert tissue-specific effects in concert with tissue-specific partner factors. In the lens, SOX2 interacts with the lens-specific factor δEF3, and this interaction is dependent on the partner-factor interaction region [16]. Y110 is also

located in this partner-factor interaction region, which is important for the cell-specific actions of SOX2. Missense mutations in this region may lead to phenotypic variability in ocular malformation and/or HH due not only to residual SOX2 activity, but also the interaction with tissue-specific partner factors.

We used a next-generation sequencing strategy to analyze 122 genes associated with congenital endocrine disorders. This approach is new in HH; it has never been reported to our knowledge. The genetic etiologies of HH are quite heterogeneous, and recent investigations have revealed that HH is not strictly a monogenic mendelian disease as previously thought; instead, it is emerging as a digenic and potentially oligogenic disease [17, 18]. When multiple genes need to be analyzed for mutations simultaneously, targeted sequence analysis of interesting genomic regions is an attractive approach.

In summary, this study expands the range of known molecular defects in SOX2, and extends our understanding of the phenotypic features and developmental disease course associated with mutations in *SOX2*.


## Acknowledgments

We thank Kazue Kinoshita for technical assistance. We also thank Professor Takao Takahashi for his fruitful discussion of our study. This work was supported by Health and Labour Sciences Research Grant for Research on Applying Health Technology [Jitsuyoka (Nanbyo) – Ippan-014].


## Disclosure Statement

The authors have nothing to disclose.

## References


1 Karges B, de Roux N: Molecular genetics of isolated hypogonadotropic hypogonadism and Kallmann syndrome. Endocr Dev 2005;8:67–80.
2 de Roux N: GnRH receptor and GPR54 inactivation in isolated gonadotropic deficiency. Best Pract Res Clin Endocrinol Metab 2006; 20:515–528.
3 Silveira LF, Trarbach EB, Latronico AC: Genetics basis for GnRH-dependent pubertal disorders in humans. Mol Cell Endocrinol 2010;324:30–38.
4 Bouligand J, Ghervan C, Tello JA, Brailly-Tabard S, Salenave S, Chanson P, Lombès M, Millar RP, Guiochon-Mantel A, Young J: Isolated familial hypogonadotropic hypogonadism and a GNRH1 mutation. N Engl J Med 2009;360:2742–2748.
5 Topaloglu AK, Reimann F, Guclu M, Yalin AS, Kotan LD, Porter KM, Serin A, Mungan NO, Cook JR, Ozbek MN, Imamoglu S, Akalin NS, Yuksel B, O'Rahilly S, Semple RK: TAC3 and TACR3 mutations in familial hypogonadotropic hypogonadism reveal a key role for neurokinin B in the central control of reproduction. Nat Genet 2009;41:354–358.
6 Topaloglu AK, Tello JA, Kotan LD, Ozbek MN, Yilmaz MB, Erdogan S, Gurbuz F, Temiz F, Millar RP, Yuksel B: Inactivating KISS1 mutation and hypogonadotropic hypogonadism. N Engl J Med 2012;366:629–635.
7 Kelberman D, Rizzoti K, Avilion A, Bitner-Glindzicz M, Cianfarani S, Collins J, Chong WK, Kirk JM, Achermann JC, Ross R, Carmignac D, Lovell-Badge R, Robinson IC, Dattani MT: Mutations within Sox2/SOX2 are associated with abnormalities in the hypothalamo-pituitary-gonadal axis in mice and humans. J Clin Invest 2006;116:2442–2455.
8 Kelberman D, de Castro SC, Huang S, Crolla JA, Palmer R, Gregory JW, Taylor D, Cavallo L, Faienza MF, Fischetto R, Achermann JC, Martinez-Barbera JP, Rizzoti K, Lovell-Badge R, Robinson IC, Gerrelli D, Dattani MT: SOX2 plays a critical role in the pituitary, forebrain, and eye during human embryonic development. J Clin Endocrinol Metab 2008; 93:1865–1873.
9 Fantes J, Ragge NK, Lynch SA, McGill NI, Collin JR, Howard-Peebles PN, Hayward C, Vivian AJ, Williamson K, van Heyningen V, FitzPatrick DR: Mutations in SOX2 cause anophthalmia. Nat Genet 2003;33:461–463.
10 Williamson KA, Hever AM, Rainger J, Rogers RC, Magee A, Fiedler Z, Keng WT, Sharkey FH, McGill N, Hill CJ, Schneider A, Messina M, Turnpenny PD, Fantes JA, van Heyningen V, FitzPatrick DR: Mutations in SOX2 cause anophthalmia-esophageal-genital (AEG) syndrome. Hum Mol Genet 2006; 15:1413–1422.
11 Schneider A, Bardakjian T, Reis LM, Tyler RC, Semina EV: Novel SOX2 mutations and genotype-phenotype correlation in anophthalmia and microphthalmia. Am J Med Genet A 2009;149A:2706–2715.
12 Leiden University Medical Center. Leiden Open Variation Database. MRC Human Genetics Unit LOVD at MRC IGMM. Leiden University Medical Center website. http://lsdb.hgu.mrc.ac.uk/home.php.
13 Woods KS, Cundall M, Turton J, Rizotti K, Mehta A, Palmer R, Wong J, Chong WK, Al-Zyoud M, El-Ali M, Otonkoski T, Martinez-Barbera JP, Thomas PQ, Robinson IC, Lovell-Badge R, Woodward KJ, Dattani MT: Over- and underdosage of SOX3 is associated with infundibular hypoplasia and hypopituitarism. Am J Hum Genet 2005;76:833–849.
14 Sato N, Kamachi Y, Kondoh H, Shima Y, Morohashi K, Horikawa R, Ogata T: Hypogonadotropic hypogonadism in an adult female with a heterozygous hypomorphic mutation of SOX2. Eur J Endocrinol 2007;156:167–171.
15 Mihelec M, Abraham P, Gibson K, Krowka R, Susman R, Storen R, Chen Y, Donald J, Tam PP, Grigg JR, Flaherty M, Gole GA, Jamieson RV: Novel SOX2 partner-factor domain mutation in a four-generation family. Eur J Hum Genet 2009;17:1417–1422.
16 Kamachi Y, Cheah KS, Kondoh H: Mechanism of regulatory target selection by the SOX high-mobility-group domain proteins as revealed by comparison of SOX1/2/3 and SOX9. Mol Cell Biol 1999;19:107–120.
17 Pitteloud N, Durrani S, Raivio T, Sykiotis GP: Complex genetics in idiopathic hypogonadotropic hypogonadism. Front Horm Res 2010; 39:142–153.
18 Sykiotis GP, Plummer L, Hughes VA, Au M, Durrani S, Nayak-Young S, Dwyer AA, Quinton R, Hall JE, Gusella JF, Seminara SB, Crowley WF Jr, Pitteloud N: Oligogenic basis of isolated gonadotropin-releasing hormone deficiency. Proc Natl Acad Sci USA 2010;34: 15140–15144.

3 Lang GH, Kagiya Y, Ohnishi-Kameyama M, Kitta K. Evaluation of extraction solutions for biochemical analyses of the proteins in rice grains. *Biosci. Biotechnol. Biochem.* 2013; **77**: 126–31.
4 Urisu A, Yamada K, Masuda S *et al.* 16-kilodalton rice protein is one of the major allergens in rice grain extract and responsible for cross-allergenicity between cereal grains in the Poaceae family. *Int. Arch. Allergy Appl. Immunol.* 1991; **96**: 244–52.
5 Usui Y, Nakase M, Hotta H *et al.* A 33-kDa allergen from rice (Oryza sativa L. Japonica). cDNA cloning, expression, and identification as a novel glyoxalase I. *J. Biol. Chem.* 2001; **276**: 11376–81.
6 Asero R, Amato S, Alfieri B, Folloni S, Mistrello G. Rice: Another potential cause of food allergy in patients sensitized to lipid transfer protein. *Int. Arch. Allergy Immunol.* 2007; **143**: 69–74.
7 Ikezawa Z, Tsubaki K, Osuna H *et al.* [Usefulness of hypoallergenic rice (AFT-R 1) and analysis of the salt insoluble rice allergen molecule]. *Arerugi* 1999; **48**: 40–9.
8 Kilshaw PJ, Heppell LM, Ford JE. Effects of heat treatment of cow's milk and whey on the nutritional quality and antigenic properties. *Arch. Dis. Child.* 1982; **57**: 842–7.
9 Sasagawa A, Yamazaki A. Development of food products using high-pressure induced transformation (Hi-pit). *Rev. High Pressure Sci. Technol.* 2008; **18**: 139–46.

# Neonatal case of classic maple syrup urine disease: Usefulness of $^1$H-MRS in early diagnosis

Takeshi Sato,[1,5] Koji Muroya,[1] Junko Hanakawa,[1] Yumi Asakura,[1] Noriko Aida,[2] Moyoko Tomiyasu,[3] Go Tajima,[4] Tomonobu Hasegawa[5] and Masanori Adachi[1]

*Departments of [1]Endocrinology and Metabolism and [2]Radiology, Kanagawa Children's Medical Center, Yokohama, [3]Research Center for Charged Particle Therapy, National Institute of Radiological Sciences, Chiba, [4]Department of Pediatrics, Hiroshima University Graduate School of Biomedical and Health Sciences, Hiroshima and [5]Department of Pediatrics, Keio University School of Medicine, Tokyo, Japan*

**Abstract** We describe a male neonate with classic maple syrup urine disease (MSUD) in metabolic crisis. On day 7 of life, he was referred to hospital because of coma and metabolic acidosis with maple syrup odor. On day 4 after admission, brain magnetic resonance imaging findings were consistent with encephalopathy due to MSUD. Proton magnetic resonance spectroscopy ($^1$H-MRS) showed a large methyl resonance peak at 0.9 p.p.m. The diagnosis of MSUD was confirmed on low branched-chain α-keto acid dehydrogenase complex activity in lymphocyte. $^1$H-MR spectra were obtained in 10 min, while it took at least several days to obtain the results of other diagnostic examinations. In convalescence, the peak at 0.9 p.p.m. decreased. The large methyl resonance peak at 0.9 p.p.m. in brain $^1$H-MRS would be one of the earliest clues to the diagnosis of classic MSUD in the neonatal period, especially in metabolic crisis.

**Key words** early diagnosis, maple syrup urine disease, metabolic crisis, neonate, proton magnetic resonance spectroscopy.

Maple syrup urine disease (MSUD; OMIM 248600) is a rare autosomal recessive inborn error of branched-chain amino acid (BCAA) metabolism.[1] The defect of the branched-chain α-keto acid dehydrogenase complex leads to the accumulation of BCAA, including leucine, valine and isoleucine, and their α-keto acids in tissues. Clinical manifestations include a maple syrup odor, mental and motor retardation, feeding problems, and convulsion. Laboratory findings include metabolic ketoacidosis, elevated plasma leucine, valine and isoleucine, sometimes hypoglycemia, hyperlactatemia and hyperammonemia. In metabolic crisis, fatal brain edema sometimes occurs. MSUD is divided into five different forms: classic; intermittent; intermediate; thiamine responsive; and dihydrolipoyl dehydrogenase (E3) deficient.

Some neonates with classic MSUD suffer from metabolic crisis within 1 week after birth,[1] before neonatal screening results are obtained. Although early diagnosis and specific treatment improve the outcome in neonates with classic MSUD,[2] it is challenging to diagnose MSUD early for two reasons. First, it is difficult for pediatricians to distinguish MSUD from common fatal diseases in the neonatal period, because patients with MSUD do not show any specific clinical manifestations except a maple syrup odor, nor specific routine laboratory findings. Second, it takes at least several days to obtain the results of diagnostic examinations, because most pediatricians cannot perform diagnostic examinations in their own laboratories.

Correspondence: Koji Muroya, MD PhD, Department of Endocrinology and Metabolism, Kanagawa Children's Medical Center, 2-138-4 Mutsukawa, Minami-ku, Yokohama-shi, Kanagawa 232-8555, Japan. Email: kmuroya@kcmc.jp

Received 5 April 2013; revised 22 July 2013; accepted 9 August 2013.
doi: 10.1111/ped.12211

Proton magnetic resonance spectroscopy ($^{1}$H-MRS) directly and non-invasively measures regional metabolite levels *in vivo*. One $^{1}$H-MRS datum can be obtained within 10 min, in addition to routine magnetic resonance imaging (MRI) of the brain. $^{1}$H-MRS has been applied to provide additional information for radiological diagnosis of neurodegenerative disorders, brain tumors and metabolic diseases.[3,4] In previous studies, $^{1}$H-MR spectra in older children with MSUD had a methyl resonance peak at 0.9 p.p.m. that increased remarkably in metabolic decompensation.[5–7] Although there is one report on $^{1}$H-MRS in neonates with classic MSUD in metabolic crisis,[5] the potential benefit of $^{1}$H-MRS in early diagnosis of classic MSUD has not been discussed.

Here, we focus on the usefulness of $^{1}$H-MRS in early diagnosis of classic MSUD in the neonatal period, especially in metabolic crisis.

## Case report

The proband, a male neonate, was the fourth child of healthy, non-consanguineous Filipino parents. An elder sister died due to metabolic crisis of MSUD at 9 years of age. The proband was delivered vaginally at term. His birthweight was 3724 g (+1.7 SD), length, 50.0 cm (+0.4 SD), and head circumference, 36.0 cm (+2.0 SD). He had been breastfed. He left the hospital on day 4 of life with his mother.

His parents noticed poor feeding and a maple syrup odor on day 6 of life. The previous doctor referred him to hospital due to metabolic acidosis on day 7 of life. On clinical examination he was in a comatose state with a bulging anterior fontanelle. Blood tests indicated normal ammonia level (72 μmol/L; reference, <110 μmol/L). Computed tomography indicated brain edema. We suspected that he suffered from metabolic crisis of MSUD based on family history and the maple syrup odor. On day 2 after admission, we started a BCAA-free formula. On day 4 after admission, MRI of the brain at 3 T showed marked restriction of proton diffusion in the thalami, the posterior limb of the internal capsule and the globus pallidus (Fig. 1a,b). In addition, $^{1}$H-MR spectra showed a large methyl peak at 0.9 p.p.m., at the left centrum–semiovale and the left basal ganglia that were obtained in 5 min each (Fig. 1c,d). A decreased *N*-acetyl aspartate (NAA) peak was also observed (Fig. 1c,d). These findings were consistent with MSUD encephalopathy. We obtained the results of neonatal screening the next day and other diagnostic examinations the next week (Table 1). The diagnosis of MSUD was confirmed by low branched-chain α-keto acid dehydrogenase complex

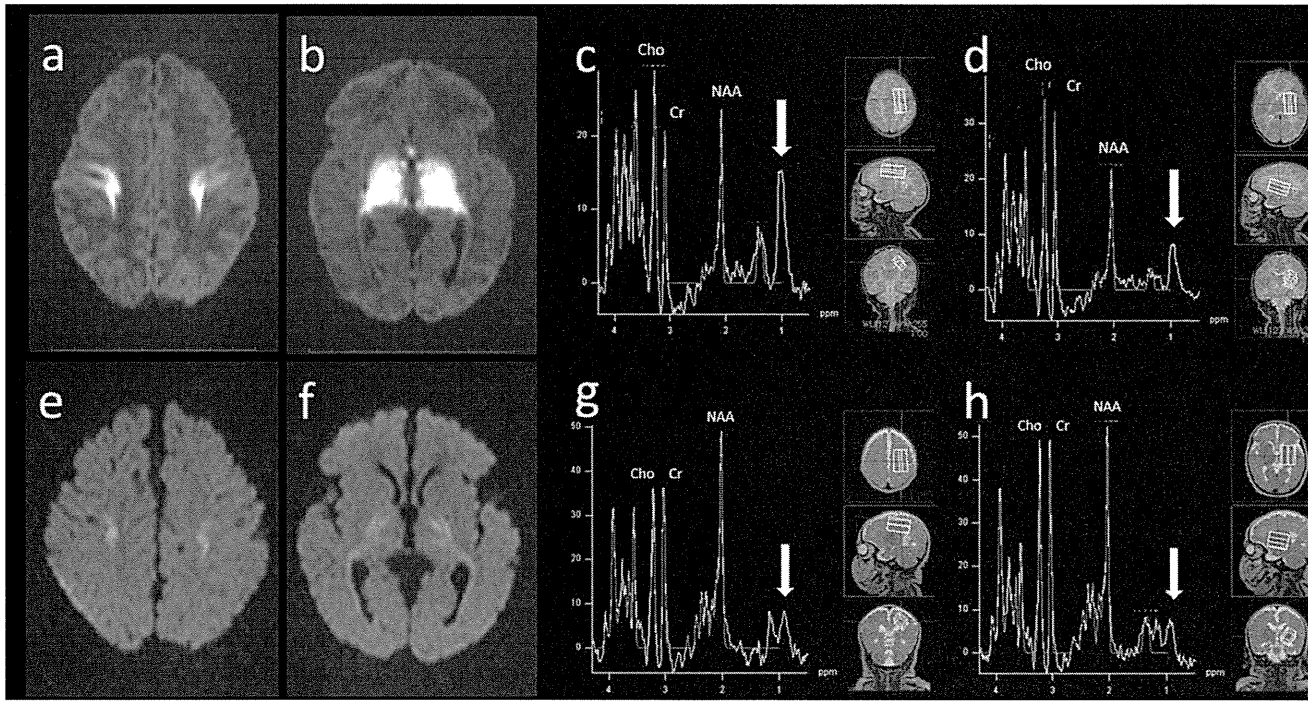


**Fig. 1** Magnetic resonance imaging and proton magnetic resonance spectroscopy ($^{1}$H-MRS) findings at (a–d) onset and in (e–h) convalescence. (a,b) Axial diffusion-weighted images (TR/TE, 6700/123 ms; section thickness, 3.0 mm; b value, 1500 s/mm$^{2}$) at (a) centrum–semiovale and (b) internal capsule. Note marked restriction of proton diffusion in the thalami, the posterior limb of the internal capsule and the globus pallidus. (c,d) $^{1}$H-MRS (TR/TE/NEX, 5000 ms/30 ms/6) at (c) the left centrum–semiovale and (d) the left basal ganglia. Note the large peak at 0.9 p.p.m. (arrows) and the decreased NAA peak. (e,f) Axial diffusion-weighted images (TR/TE, 7200/120 ms; section thickness, 3.0 mm; b value, 1500 s/mm$^{2}$) at (e) centrum–semiovale and (f) internal capsule. Note the significant resolution of the hyperintense lesions. (g,h) $^{1}$H-MRS (TR/TE/NEX, 5000 ms/30 ms/6) at (g) the left centrum–semiovale and (h) the left basal ganglia. Note the decreased peak at 0.9 p.p.m. (arrows) and the increased NAA peak. The Cr level in convalescence was higher than the one at the onset. Cho, choline; Cr, creatine; NAA, *N*-acetyl aspartate; NEX, no. excitations; TE, echo time; TR, repetition time.

**Table 1** Diagnostic examinations

| Diagnostic examinations | Results (local references) | | | Time required for results |
|---|---|---|---|---|
| Neonatal screening by high performance liquid chromatography | Leucine | 21.1 (<3.5) | mg/dL | 7 days |
| Plasma amino acid analysis by liquid chromatography mass spectrometry | Leucine | 3218.6 (76.6–171.3) | nmol/mL | 12 days |
| | Valine | 1076.1 (147.8–307.0) | nmol/mL | |
| | Isoleucine | 1000.4 (43.0–112.8) | nmol/mL | |
| Urine organic acid analysis | High levels of α-keto and hydroxyl acids | | | 13 days |
| Branched-chain α-keto acid dehydrogenase complex activity in lymphocyte | 0.14 (3.89–7.43) | pmol isovaleryl-CoA/min/$10^6$ lymphocytes | | 3 days |

activity in lymphocyte (Table 1). In spite of intensive treatment with BCAA-free formula through the nasogastric tube and parenteral high-caloric nutrition with insulin, he developed a high ammonia level (218 μmol/L) and needed continuous arteriovenous hemofiltration on day 24 after admission. He then made satisfactory progress. In convalescence at 2 months of age, MRI indicated significant resolution of the hyperintense lesions (Fig. 1e,f). On $^1$H-MRS the peak at 0.9 p.p.m. had decreased and the NAA peak had increased (Fig. 1g,h; Table 2). The creatine (Cr) level in convalescence was higher than that at onset (Fig. 1; Table 2). On day 157 after admission, he left hospital, using the nasogastric tube. He managed to drink milk from a bottle at 6 months of age. He started babbling and pulling himself up at 16 months of age.

## Discussion

We have described a male neonate with classic MSUD in metabolic crisis. Based on his family history and the maple syrup odor, we started BCAA-free formula, before we obtained the results of other diagnostic examinations. Brain $^1$H-MRS showed a large methyl resonance peak at 0.9 p.p.m. characteristic for MSUD, at the left centrum–semiovale and the left basal ganglia in 5 min each. In contrast, it took at least several days to obtain the results of other diagnostic examinations, including neonatal screening, plasma amino acid analysis, urine organic acid analysis and enzymatic activity. Retrospectively, we believe that the large methyl resonance peak at 0.9 p.p.m. on brain $^1$H-MRS would be one of the earliest clues to the diagnosis of classic MSUD in the neonatal period, especially in metabolic crisis.

In MSUD the peak at 0.9 p.p.m. is larger than the one at 1.3 p.p.m. on $^1$H-MRS of the brain. In MSUD patients, the large peak at 0.9 p.p.m. is thought to originate from BCAA and/or their derivatives, which have more methyl groups (-$CH_3$ at 0.9 p.p.m.) than methylene groups (-$CH_2$- at 1.3 p.p.m.).[7] We must interpret the peaks at 0.9 p.p.m. and 1.3 p.p.m. with caution, because the resonance at 0.9 p.p.m. and 1.3 p.p.m. is not specific to MSUD. Several disorders, such as Sjögren–Larsson syndrome, have prominent lipid peaks at both 0.9 p.p.m. and 1.3 p.p.m.[8] Hyperlactatemia, which often occurs in metabolic crisis of MSUD, can also be confused with the peak at 1.3 p.p.m. Fortunately, it is not difficult to exclude other diseases based on medical history, physical examinations and routine laboratory examinations.

We could not determine whether the NAA and Cr levels increased in convalescence due to therapeutic response or to age-dependent changes (Table 2). NAA is considered to be a marker of neuronal density or mitochondrial metabolic function.[9] A decreased NAA peak could be observed in metabolic disorders.[4] It is also well known, however, that NAA concentration increases with development.[10] Cr level is reported to be relatively stable, but may change with development or tissue damage.[4] We observed that the choline (Cho) level remained almost unchanged (Table 2). Although Cho is known to be involved in cell membrane metabolism and myelination,[4] the significance of the Cho level remained unknown in MSUD. In contrast, the decreased peak at 0.9 p.p.m. might have reflected decreased BCAA and/or their α-keto acids directly. $^1$H-MRS in the present neonatal patient showed a decreased peak at 0.9 p.p.m. in convalescence at 2 months of age, compared with the one at onset (Fig. 1; Table 2). Previous studies showed that the peak at 0.9 p.p.m. decreased in convalescence in older children.[5] Thus, among the peaks of the major metabolites, such as NAA, Cr and Cho, the peak at 0.9 p.p.m. would be the most useful to estimate the efficacy of treatment regardless of patient age.

### *Conclusion*

We have demonstrated the usefulness of $^1$H-MRS at the centrum-semiovale and the basal ganglia in early diagnosis of classic

**Table 2** Metabolite concentrations

| | -$CH_3$ (at 0.9 p.p.m.)† | | *N*-acetyl aspartate | | Choline | | Creatine | |
|---|---|---|---|---|---|---|---|---|
| | CS | BG | CS | BG | CS | BG | CS | BG |
| Onset (mmol/L) | 11.3 | 6.3 | 2.7 | 2.7 | 1.3 | 1.9 | 3.4 | 5.1 |
| Convalescence (mmol/L) | 6.0 | 4.9 | 4.8 | 5.1 | 1.5 | 1.8 | 5.5 | 6.8 |

Quantification of metabolite concentrations were derived using LCModel software. †mmol/L of $CH_3$ groups. BG, basal ganglia; CS, centrum–semiovale.

MSUD in the neonatal period, especially in metabolic crisis. Classic MSUD may be able to be distinguished from other serious illnesses and specific treatment initiated immediately, when $^{1}$H-MRS findings are interpreted in combination with the clinical course, physical examinations, routine laboratory findings and routine MRI findings.

## Acknowledgments

We thank the family for participating in this study. We also thank Drs Takahiro Murata and Akira Ishiguro for providing us with clinical information, and Dr Satoshi Narumi for fruitful discussion and critical reading of the manuscript.

## References

1 Morton DH, Strauss KA, Robinson DL, Puffenberger EG, Kelley RI. Diagnosis and treatment of maple syrup disease: A study of 36 patients. *Pediatrics* 2002; **109**: 999–1008.
2 Naughten ER, Jenkins J, Francis DE, Leonard JV. Outcome of maple syrup urine disease. *Arch. Dis. Child.* 1982; **57**: 918–21.
3 Wang Z, Zimmerman RA, Sauter R. Proton MR spectroscopy of the brain: Clinically useful information obtained in assessing CNS diseases in children. *AJR Am. J. Roentgenol.* 1996; **167**: 191–9.
4 Wang ZJ, Zimmerman RA. Proton MR spectroscopy of pediatric brain metabolic disorders. *Neuroimaging Clin. N. Am.* 1998; **8**: 781–807.
5 Jan W, Zimmerman RA, Wang ZJ, Berry GT, Kaplan PB, Kaye EM. MR diffusion imaging and MR spectroscopy of maple syrup urine disease during acute metabolic decompensation. *Neuroradiology* 2003; **45**: 393–9.
6 Felber SR, Sperl W, Chemelli A, Murr C, Wendel U. Maple syrup urine disease: Metabolic decompensation monitored by proton magnetic resonance imaging and spectroscopy. *Ann. Neurol.* 1993; **33**: 396–401.
7 Heindel W, Kugel H, Wendel U, Roth B, Benz-Bohm G. Proton magnetic resonance spectroscopy reflects metabolic decompensation in maple syrup urine disease. *Pediatr. Radiol.* 1995; **25**: 296–9.
8 Tachibana Y, Aida N, Enomoto K, Iai M, Kurosawa K. A case of Sjögren-Larsson syndrome with minimal MR imaging findings facilitated by proton spectroscopy. *Pediatr. Radiol.* 2012; **42**: 380–82.
9 Govindaraju V, Young K, Maudsley AA. Proton NMR chemical shifts and coupling constants for brain metabolites. *NMR Biomed.* 2000; **13**: 129–53.
10 Kreis R, Hofmann L, Kuhlmann B, Boesch C, Bossi E, Hüppi PS. Brain metabolite composition during early human brain development as measured by quantitative in vivo $^{1}$H magnetic resonance spectroscopy. *Magn. Reson. Med.* 2002; **48**: 949–58.

# Two children with obesity-related glomerulopathy identified in a school urinary screening program

Yukihiko Kawasaki, Masato Isome, Atsushi Ono, Yuichi Suzuki, Kei Takano, Kazuhide Suyama and Mitsuaki Hosoya
*Department of Pediatrics, Fukushima Medical University School of Medicine, Fukushima, Japan*

**Abstract** The incidence of obesity-related glomerulopathy (ORG) has increased over the last decade, but there have been few reports on ORG in Japanese children. Reported herein are two children with ORG identified on school urinary screening (SUS). Patient 1 was a 12-year-old boy in whom proteinuria was first detected on SUS. His body mass index (BMI) was 33.8 kg/m$^2$ and he had hypertension and hyperuricemia. Patient 2, a 10-year-old boy, also had proteinuria identified on SUS. His BMI was 34.8 kg/m$^2$, and he had fatty liver, hyperuricemia, and hypercholesterolemia. Both were diagnosed with ORG based on obesity, proteinuria, and renal pathological findings. After treatment, including candesartan, food restriction and physical exercise, urinary protein excretion was decreased in both cases. We believe that such school urinary screening programs may be effective for the early identification and treatment of children with ORG.

**Key words** angiotensin II receptor blocker child, focal segmental glomerulosclerosis, obesity-related glomerulopathy, school urinary screening.

Obesity is a major health problem, and its incidence is increasing worldwide.[1] In Japan, the prevalence of obesity has been consistently increasing in men, whereas it has been stable over the last 10 years in women: according to the annual report of the National Nutrition Survey, Japan, currently, the prevalence of overweight is 30.9% in men and 22.7% in women aged ≥20 years.[2] Mitsuhashi *et al.* observed that the prevalence of overweight was 3.12% among children aged 6 years in 1985, and it steadily increased to 4.68% in 2005.[3]

A particular form of kidney disease, so-called obesity-related glomerulopathy (ORG), is characterized by glomerulomegaly with or without focal segmental glomerulosclerosis (FSGS), and the incidence of ORG has increased during the last decade with

Correspondence: Yukihiko Kawasaki, MD PhD, Department of Pediatrics, Fukushima Medical University School of Medicine, 1 Hikarigaoka, Fukushima City, Fukushima 960-1295, Japan. Email: kyuki@fmu.ac.jp

Received 4 March 2013; revised 19 May 2013; accepted 23 August 2013.
doi: 10.1111/ped.12213

Pituitary
DOI 10.1007/s11102-013-0546-5

# A novel mutation in *SOX3* polyalanine tract: a case of kabuki syndrome with combined pituitary hormone deficiency harboring double mutations in *MLL2* and *SOX3*

**Masaki Takagi · Tomohiro Ishii · Chiharu Torii · Kenjiro Kosaki · Tomonobu Hasegawa**



**Abstract**
*Introduction* Both duplications encompassing *SOX3* and loss-of function mutations in *SOX3* have been reported in a minor portion of X-linked isolated growth hormone deficiency (GHD) or combined pituitary hormone deficiency (CPHD) patients with or without mental retardation.
*Patients and methods* We report a Japanese male patient with molecularly confirmed Kabuki syndrome who was found to have CPHD. We analyzed all coding exons and flanking introns of currently known nine genes responsible for CPHD by PCR-based sequencing.
*Results* In this CPHD patient, we identified a novel hemizygous 21-base pair deletion, resulting in the loss of 7 alanine residues from polyalanine (PA) tracts of *SOX3*. The clinically and endocrinologically normal mother of the patient carried the same deletion in a heterozygous manner. In vitro experiments showed that the del 7A SOX3 had increased transactivation of the *HESX1* promoter.
*Conclusion* Our study provides additional evidence that deletion in PA tracts of *SOX3* is associated with hypopituitarism. Female carriers of *SOX3* PA tract deletions will show a broad phenotypic spectrum, ranging from clinically normal to CPHD.

M. Takagi · T. Ishii · T. Hasegawa (✉)
Department of Pediatrics, Keio University School of Medicine, 35 Shinanomachi, Shinjuku-ku, Tokyo 160-8582, Japan
e-mail: thaseg@a6.keio.jp

M. Takagi
Department of Endocrinology and Metabolism, Tokyo Metropolitan Children's Medical Center, Tokyo, Japan

C. Torii · K. Kosaki
Center for Medical Genetics, Keio University School of Medicine, Tokyo, Japan

Published online: 18 December 2013

**Keywords** CPHD · SOX3 · PA tract

## Introduction

*SOX3* (OMIM#313430) is a member of the SOX (SRY related high mobility group box) family of transcription factors, expressed in neuroepithelial progenitor and stem cells from the earliest stages of development and its dosage is critical for normal pituitary development [1]. SOX3 contains a high mobility group DNA-binding domain, and 4 polyalanine (PA) tracts shown to be involved in transcriptional activation. Both duplications encompassing *SOX3* and loss-of function mutations in *SOX3* have been reported in a minor portion of X-linked isolated growth hormone deficiency (GHD) or combined pituitary hormone deficiency (CPHD) patients with or without mental retardation [2–5]. Here, we report the case of a Japanese patient with Kabuki syndrome (OMIM#147920, KS), who exhibited CPHD, harboring double mutations in *MLL2* and *SOX3*.

KS is a multiple congenital anomaly/intellectual disability syndrome characterized by a distinct dysmorphic facial appearance [6, 7]. Recently, mutations in *MLL2* gene (OMIM# 602113), encoding an H3K4 histone methyl transferase, which acts as an epigenetic transcriptional activator during growth and development, have been reported to be the cause of KS [8]. Endocrinological abnormalities, except for premature thelarche, are rare (or not well described) in KS. To date, GHD has been identified in very few cases [9–14]. To the best of our knowledge, no CPHD has been reported in a KS case. The lack of previous reports on this specific combination of relatively rare conditions led us to perform a genetic screen of 9 currently known CPHD-associated genes, and we identified a novel hemizygous 21-base pair deletion resulting in the

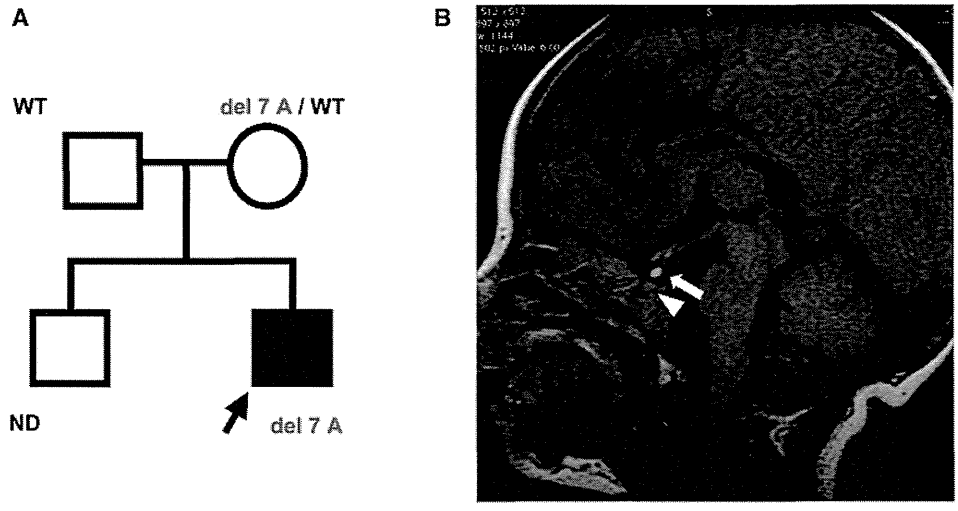


**Fig. 1** Features of the propositus. **a** The pedigrees of the family. The *arrow* indicates the propositus. **b** Brain magnetic resonance imaging (*MRI*) at the age of 3 months. An ectopic posterior gland (*arrow*) and a small anterior pituitary (*arrowhead*) are shown

loss of 7 alanine residues between codons 239 and 245 (p.Ala239_245 del 7 A) from the first PA tract of *SOX3*. Our study provides additional evidence that deletion in the first PA tract of SOX3 is associated with hypopituitarism.

## Materials and methods

### Patient report

The propositus was a 5-year-old Japanese boy born at 37 weeks of gestation after an uncomplicated pregnancy and delivery. The parents were nonconsanguineous and phenotypically normal. He had 1 older brother, who had no relevant clinical problems (Fig. 1a). His birth weight was 2,738 g (−0.7 SD), and the length was 45.0 cm (−1.9 SD). The Apgar scores were 6 and 7 at 1 and 5 min, respectively. At birth, several dysmorphic features including eversion of the lower lateral eyelid, arched eyebrows with the lateral one-third sparse, depressed nasal tip, and prominent ears were observed. At 1 week of age, he was diagnosed with congenital heart disease, including a ventriculoseptal defect, an atrial septal defect, and mitral stenosis. He exhibited postnatal growth retardation and a developmental delay. He could not sit unassisted until the age of 23 months. Severe mental retardation, with a developmental quotient (DQ) of 49, was noted at the age of 2 years. An ABR examination revealed a hearing loss: 60 dB on the right side and 50 dB on the left side at the age of 2 years. A skeletal survey revealed sagittal cleft of vertebral body. His G-banded karyotype was normal. He was diagnosed with KS.

As a neonate, he was diagnosed with central hypothyroidism on the basis of a low free T4 (0.52 ng/dL: Ref. 0.99–1.91) with an inadequately increased TSH level of 6.27 mU/L (Ref. 0.77–7.3). There was no micropenis or undescended testes. Prolonged cholestasis and frequent episodes of hypoglycemia were noted at the age of 2 months. He was diagnosed with cortisol deficiency on the basis of low cortisol (10.9 μg/dL) at the time of severe hypoglycemia (glucose 0.9 mmol/L). Brain magnetic resonance imaging (MRI) at the age of 3 months showed a small anterior pituitary with a visible stalk, and an ectopic posterior pituitary gland (EPP) (Fig. 1b). As an extra pituitary finding, a hypoplastic corpus callosum was noted. Replacement therapy with l-thyroxine and hydrocortisone was started at 1 and 7 months of age, respectively. At the age of 2 years, his height and weight were 72.0 cm (−5.1 SD) and 8.0 kg (−3.3 SD) respectively. He presented with persistent hypoglycemia, low serum concentrations of IGF-I, and impaired GH response on arginine hydrochloride testing (peak GH 3.2 ng/mL, Ref. >6.0), and replacement therapy with recombinant human GH was started. After starting GH therapy, hypoglycemia has not been recorded. Follow-up MRI at the age of 2 years showed anterior pituitary hypoplasia, poorly developed sella turcica, a visible, but thin stalk, and EPP. Basal prolactin concentration was 6.9 and 3.9 ng/mL at the ages of 1, 2 years respectively.

### Mutation analysis of *MLL2* gene and the genes responsible for CPHD

After genetic counseling, we obtained written informed consent from the patient or parents for molecular studies, which were approved by the Institutional Review Board of the Keio University School of Medicine. Genomic DNAs were extracted from peripheral blood of the patients and parents by using standard techniques. We analyzed all the coding exons and flanking introns of *MLL2*. For genetic screening of CPHD, we analyzed all coding exons and flanking introns of *POU1F1, PROP1, HESX1, LHX3, LHX4, OTX2, SOX2, GLI2,* and *SOX3* by PCR-based sequencing. We screened for deletion/duplication involving

*POU1F1, PROP1, HESX1, LHX3,* and *LHX4* by MLPA analyses (SALSA MLPA KIT P216; MRC-Holland, Amsterdam, The Netherlands). We tested detected sequence variation against 100 (male 65, female 35) Japanese control subjects.

X-inactivation studies

The X-chromosome inactivation pattern of the unaffected mother was determined using the androgen receptor (*AR*) gene methylation assay [15]. In brief, leukocyte genomic DNA was PCR amplified with a fluorescent labeled forward primer and an unlabeled reverse primer flanking the CAG repeat region and the two methylation sensitive *Hpa*II sites at exon 1 of *AR*, before and after *Hpa*II digestion. PCR products were obtained from both active and inactive X chromosomes before *Hpa*II digestion and from inactive X chromosomes alone after *Hpa*II digestion. For the X-inactivation analysis, the PCR products obtained before and after *Hpa*II digestion were determined for size and examined for area under curve (AUC) on an ABI PRISM 3100 autosequencer using GeneScan (Applied Biosystems, Norwalk, CT). The X inactivation ratio was calculated using the area under curve.

Functional studies

To generate SOX3 expression vectors, the S*OX3* coding region was amplified from patients' and control DNA and cloned into pCMV-myc (Clontech, Palo Alto, CA). A luciferase reporter vector was constructed by inserting the *HESX1* promoter sequence (−405 to +267 bp) into a pGL4.24 [luc2P/minP] vector (Promega, Madison, WI). A transactivation assay was performed in COS1 cells using a dual-luciferase reporter assay system (Promega). For subcellular localization analyses, COS1 cells transfected with the myc-tagged SOX3 were fixed in 4 % paraformaldehyde, permeabilized with 0.2 % TritonX-100 and blocked in 10 % BSA in PBS. Cells were then incubated with a mouse anti-myc monoclonal antibody (Invitrogen) for 1 h. After washing, cells were incubated with 1:1,000 Alexa Fluor secondary antibodies (Cell Signaling Technology) in blocking buffer for 1 h. Cells were imaged using an IX-71 fluorescence microscope (Olympus, Tokyo, Japan). For immunoblot assays, COS1 cells transfected with the myc-tagged SOX3 were harvested, and nuclear protein was isolated with the NE-PER nuclear extraction reagent kit (Pierce, Rockford, IL). Western blotting was performed with a mouse anti-myc monoclonal antibody (Invitrogen).

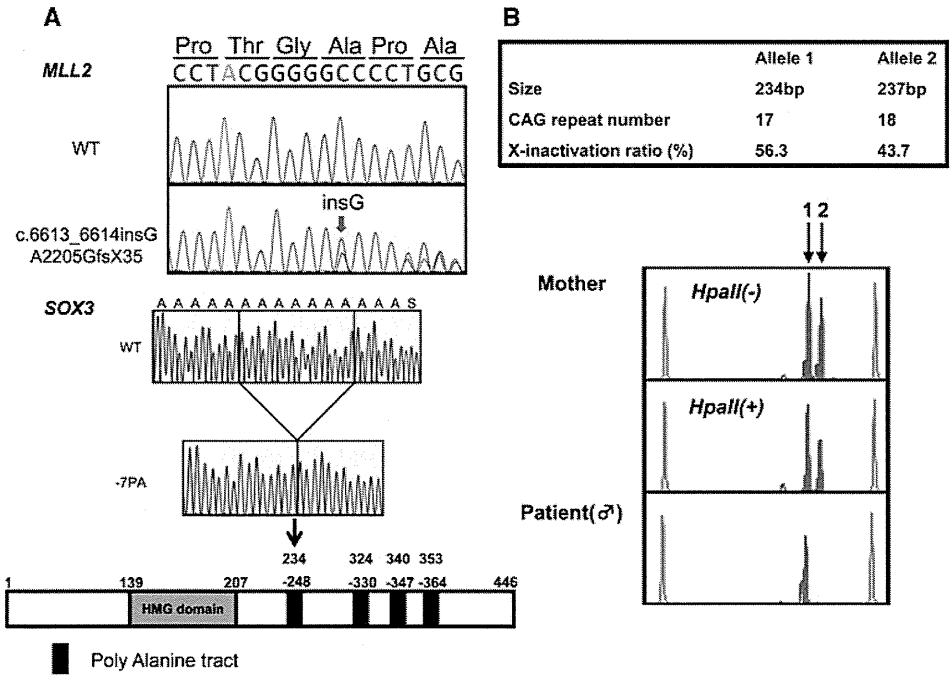


**Fig. 2** Identification of mutations in *MLL2* and *SOX3*. **a** The *red arrow* indicates the mutation in *MLL2*. **b** We identified a hemizygous novel 21-base pair in-frame deletion, resulting in the loss of seven alanine residues between codons 239 and 245 (p.Ala239_245 del7A) of *SOX3*. **c** CAG repeat length and X-inactivation analyses. Before *Hpa*II digestion, two alleles have been delineated on the autosequencer. Allele 1, which represents mutated allele, is 234 bp long and contains 17 CAG repeats, and allele 2 is 237 bp long and contains 18 CAG repeats. The X-inactivation ratio is calculated using the AUCs before and after *Hpa*II digestion. In the mother, allele 1 is preferentially inactivated compared with allele 2 (Allele 1: 56.3 %, Allele 2: 43.7 %)

The sequences of the biotin-labeled double stranded oligonucleotide used as probe in the EMSA experiment was 5′-CAAACAAATAAACAATTAACTC-3′ [3]. Five microgram of nuclear protein extraction was incubated at room temperature in 20-μL binding reaction mixture contained 20 fmol probe, 50 mM KCl, 5 mM $MgCl_2$, 2.5 % glycerol, 0.05 % NP-40, and 1 μg poly (dI–dC) for 20 min. For competition experiments, a large excess (200×) of unlabeled competitor oligonucleotides was included in the binding reactions. The protein-DNA complexes were subject to gel electrophoresis and transferred to a nylon membrane. The biotin-labeled probe was detected with the Lightshift chemiluminescent EMSA kit (Pierce).

## Results

### Mutation analysis of *MLL2* gene and the genes responsible for CPHD

We identified a novel heterozygous frameshift mutation in *MLL2*, namely c.6613_6614insG, p.Ala2205GlyfsX38 (Fig. 2a). Familial gene analysis revealed that this mutation was de novo.

We also identified a hemizygous novel 21-base pair in-frame deletion, resulting in the loss of seven alanine residues between codons 239 and 245 (p.Ala239_245 del7A) of *SOX3* (Fig. 2b). This mutation was not detected in any of the 100 healthy controls and was absent from database, including dbSNP, the 1,000 Genomes Project, and Exome Variant Server, NHLBI Exome Sequencing Project. We detected no gross or exon-level deletions/duplications by the MLPA analyses. Genetic analyses showed that the clinically normal mother, whose adult height was 155.0 cm (−0.58 SD), carried the same 21-base pair deletion in a heterozygous manner and that the father did not. Baseline hormonal data (Table 1) and MRI findings of the mother were normal. No other family member was available for genetic studies.

**Table 1** Endocrinological findings (baseline) in the mother

| | Mother | Reference (adult) |
|---|---|---|
| GH (ng/mL) | 0.2 | 0–23 |
| IGF-1 (ng/mL) | 135.0 | Female: 73–542 |
| TSH (μU/mL) | 1.62 | 0.3–3.50 |
| Free T4 (ng/dL) | 1.2 | 1.09–2.55 |
| Free T3 (pg/mL) | 2.6 | 3.23–5.11 |
| LH (mIU/mL) | 7.8 | Female: 1.4–15[a] |
| FSH (mIU/mL) | 24.0 | Female: 3–10[a] |
| PRL (ng/mL) | 8.8 | Female: 1.4–14.6 |
| ACTH (pg/mL) | 15.0 | 7.2–63.3 |
| Cortisol (μg/dL) | 11.6 | 7.6–21.4 |
| Estradiol (pg/mL) | 20 | Female: 11–230[a] |

[a] Follicular phase

### X-inactivation studies

Preferential inactivation of the abnormal X-chromosome was shown (Fig. 2c).

### *Functional studies*

In COS1 cells, WT SOX3 stimulated transcription of the *HESX1* reporter. The del 7 PA SOX3 mutant proteins had increased transactivation compared with WT SOX3 (Fig. 3a). Subcellular localization and western blotting

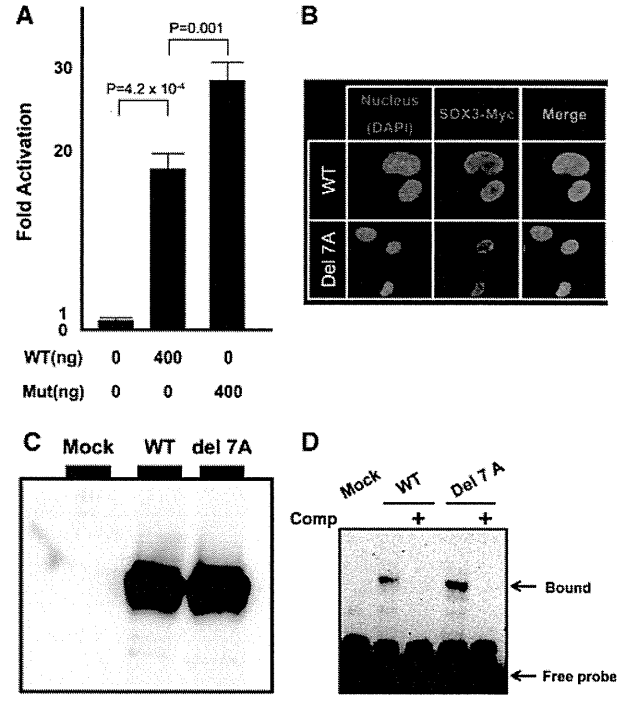


**Fig. 3** Functional characterization of del 7 A SOX3. **a** Transactivation assays of del 7 A SOX3 using *HESX1* reporter COS1 cells were cotransfected with the pRL-CMV internal control vector, indicated amount (nanograms) of the effector plasmids, and the *HESX1* reporter. WT SOX3 stimulated transcription of the *HESX1* reporter. The del 7 PA SOX3 resulted in an approximately 1.5-fold increase in transcriptional activation compared with WT SOX3 ($p = 0.001$). The data are mean ± SEM of at least three independent experiments performed in triplicate transfections. **b** Subcellular localization analysis. We visualized and photographed COS1 cells transfected with myc-tagged SOX3 using an IX-71 fluorescence microscope, after mounting the cells in Vectashield-DAPI solution. The WT and del 7 A SOX3 are localized to the nucleus. **c** Western blot analysis showed that the expression of del 7 A SOX3 was comparable to that of the WT. **d** EMSA experiments WT SOX3 showed specific binding to the elements, which was competed by excess amount of (200 times) cold competitors. The del 7 A SOX3 bound with similar or slightly high efficiency to the WT SOX3

**Table 2** Summary of the clinical phenotypes and MRI findings of *SOX3* mutations

| Case | Age at evaluation | Sex | Clinical findings | Affected pituitary hormones | MRI findings | SOX3 mutation | Ref |
|---|---|---|---|---|---|---|---|
| I-1 | 3.0 (years) | Male | Short stature (−3.0 SD)<br>Normal intelligence | GH | NA | +7 PA | 5 |
| I-2 | 1.5 (years) | Male | Short stature (−2.7 SD)<br>Learning difficulties | GH | APH<br>EPP | | |
| II-1 | 9 (years) | Male | Short stature (−2.8 SD)<br>Normal intelligence | GH | Normal AP<br>EPP | +7 PA | 4 |
| II-2 | 12 (months) | Male | Normal intelligence | GH | APH<br>EPP | | |
| III-1 | 3.0 (years) | Male | Short stature (−2.5 SD)<br>Normal intelligence | GH, TSH, LH/FSH, ACTH | NA | +7 PA | 3 |
| III-2 | 4.5 (years) | Male | Short stature (−2.5 SD)<br>Normal intelligence | GH, TSH, LH/FSH, ACTH | APH<br>EPP | | |
| III-3 | 2.7 (years) | Male | Short stature (−1.3 SD) | GH, TSH, LH/FSH, ACTH | APH<br>EPP | | |
| IV | | Male | Short stature<br>Mental retardation | GH | NA | +11 PA | 2 |
| V | | Male | Short stature<br>Mental retardation | No pituitary phenotype | NA | del 9 PA | 2 |
| VI | 7.5 (years) | Female | Short stature (−3.1 SD)<br>Normal intelligence | GH, TSH, LH/FSH | Enlarged AP<br>NPP | del 6 PA | 5 |
| Our case | 5.0 (years) | Male | Short stature<br>Mental retardation | GH, TSH, ACTH | APH<br>EPP | del 7 PA | |

*AP* anterior pituitary, *APH* anterior pituitary hypoplasia, *EPP* ectopic posterior pituitary, *NPP* normal posterior pituitary, *NA* not available

revealed no significant difference between WT and mutant SOX3 (Fig. 3b, c), indicating that protein expression and nuclear targeting were not affected by the mutation. WT SOX3 showed specific binding to the elements, which was competed by excess amount of (200 times) cold competitors. The del 7 A SOX3 bound with similar or slightly high efficiency to the WT SOX3 (Fig. 3d).

## Discussion

To date, 4 intragenic mutations in *SOX3* have been reported and all of them involve expansions or deletions of the first PA tract [2–5]. Here, we summarize the clinical phenotypes and MRI findings of *SOX3* mutations reported thus far (Table 2). At least 3 pedigrees harboring 7 alanine expansions (+7 PA) have been reported and their clinical phenotype or MRI findings have been shown to be variable among patients with the same *SOX3* mutation. In contrast to PA expansions, deletions are even rarer. A 9-alanine deletion (del 9 PA) in 2 brothers with mental retardation, but without a clearly defined pituitary phenotype and a 6-alanine deletion (del 6 PA) in a female patient with CPHD have been reported. Our case is the third report of a PA tract deletion, which had increased transactivation of SOX3 target genes as previously described by Alatzoglou et al. [5]. We believe that our observation will provide additional evidence that deletion in the PA tracts of *SOX3* is associated with hypopituitarism and will provide clinical information to extend the phenotypic spectrum of patients with PA tract deletion of *SOX3*.

A female patient with a heterozygous del 6 PA exhibited CPHD, without skewed X inactivation in the genomic DNA extracted from her peripheral blood [5]. On the other hand, the mother of our patient, carrying a del 7 PA in a heterozygous manner, was clinically and endocrinologically normal, which may be partially due to skewed X-inactivation. This indicates that female carriers of *SOX3* PA tract deletion mutations will show a broad phenotypic spectrum, from clinically normal to CPHD.

Approximately 55–80 % of KS patients are estimated to have mutations in the *MLL2* gene, encoding a large 5,537-residue protein including 7 PHD fingers, FYRN, FYRC, and a SET domain [8, 16–19]. The SET domain of MLL2 confers strong histone 3 lysine 4 methyltransferase activity and is important in the epigenetic control of active chromatin states [20]. The c.6613_6614insG mutation in *MLL2* results in a premature termination codon (PTC) with mRNA that is predicted to be destroyed by the process of nonsense-mediated RNA decay. If translated, this abnormal

transcript would generate a protein lacking one of the 7 PHD fingers, the entire of the FYRN, FYRC, and SET domain. Additionally, the de novo *MLL2* mutation of our patient indicates that the occurrence of KS and *SOX3* associated CPHD is a coincidence.

In summary, we report the case of a KS patient with CPHD, carrying mutations in *MLL2* and *SOX3*. Our study provides additional evidence that deletion in the PA tracts of *SOX3* is associated with hypopituitarism.

**Acknowledgments** We thank the patient and his family for participation in this study. We thank Kazue Kinoshita for technical assistance. This work was supported by a Grant-in-Aid for the Health Science Research Grant for Research on Applying Health Technology [Jitsuyoka (Nanbyo)-Ippan-014 (23300102)] from the Ministry of Health, Labour and Welfare of Japan.

**Conflict of interest** The authors have declared no conflicts of interest.

## References

1. Collignon J, Sockanathan S, Hacker A, Cohen-Tannoudji M, Norris D, Rastan S, Stevanovic M, Goodfellow PN, Lovell-Badge R (1996) A comparison of the properties of SOX-3 with Sry and two related genes, Sox-1 and Sox-2. Development 122(2):509–520
2. Laumonnier F, Ronce N, Hamel BC, Thomas P, Lespinasse J, Raynaud M, Paringaux C, Van Bokhoven H, Kalscheuer V, Fryns JP, Chelly J, Moraine C, Briault S (2002) Transcription factor SOX3 is involved in X-linked mental retardation with growth hormone deficiency. Am J Hum Genet 71(6):1450–1455
3. Woods KS, Cundall M, Turton J, Rizotti K, Mehta A, Palmer R, Wong J, Chong WK, Al-Zyoud M, El-Ali M, Otonkoski T, Martinez-Barbera JP, Thomas PQ, Robinson IC, Lovell-Badge R, Woodward KJ, Dattani MT (2005) Over- and underdosage of SOX3 is associated with infundibular hypoplasia and hypopituitarism. Am J Hum Genet 76(5):833–849
4. Burkitt Wright EM, Perveen R, Clayton PE, Hall CM, Costa T, Procter AM, Giblin CA, Donnai D, Black GC (2009) X-linked isolated growth hormone deficiency: expanding the phenotypic spectrum of *SOX3* polyalanine tract expansions. Clin Dysmorphol 18(4):218–221
5. Alatzoglou KS, Kelberman D, Cowell CT, Palmer R, Arnhold IJ, Melo ME, Schnabel D, Grueters A, Dattani MT (2011) Increased transactivation associated with *SOX3* polyalanine tract deletion in a patient with hypopituitarism. J Clin Endocrinol Metab 96(4):685–690
6. Niikawa N, Matsuura N (1981) Kabuki make-up syndrome: a syndrome of mental retardation, unusual facies, large and protruding ears, and postnatal growth deficiency. J Pediatr 99(4):565–569
7. Kuroki Y, Suzuki Y, Chyo H, Hata A, Matsui I (1981) A new malformation syndrome of long palpebral fissures, large ears, depressed nasal tip, and skeletal anomalies associated with postnatal dwarfism and mental retardation. J Pediatr 99(4):570–573
8. Ng SB, Bigham AW, Buckingham KJ, Hannibal MC, McMillin MJ, Gildersleeve HI, Beck AE, Tabor HK, Cooper GM, Mefford HC, Lee C, Turner EH, Smith JD, Rieder MJ, Yoshiura K, Matsumoto N, Ohta T, Niikawa N, Nickerson DA, Bamshad MJ, Shendure J (2010) Exome sequencing identifies *MLL2* mutations as a cause of Kabuki syndrome. Nat Genet 42(9):790–793
9. Niikawa N, Kuroki Y, Kajii T, Matsuura N, Ishikiriyama S, Tonoki H, Ishikawa N, Yamada Y, Fujita M, Umemoto H (1988) Kabuki make-up (Niikawa-Kuroki) syndrome: a study of 62 patients. Am J Med Genet 31(3):565–589
10. Handa Y, Maeda K, Toida M, Kitajima T, Ishimaru J, Nagai A, Oka N (1991) Kabuki make-up syndrome (Niikawa-Kuroki syndrome) with cleft lip and palate. J Craniomaxillofac Surg 19(3):99–101
11. Satoh M, Arakawa K, Yokoya S, Morooka K (1993) A case of Kabuki make-up syndrome associated with growth hormone deficiency. Clin Pediatr Endocrinol 2(1):13–16
12. Tawa R, Kaino Y, Ito T, Goto Y, Kida K, Matsuda H (1994) A case of Kabuki make-up syndrome with central diabetes insipidus and growth hormone neurosecretory dysfunction. Acta Paediatr Jpn 36(4):412–415
13. Devriendt K, Lemli L, Craen M, de Zegher F (1995) Growth hormone deficiency and premature thelarche in a female infant with kabuki makeup syndrome. Horm Res 43(6):303–306
14. Gabrielli O, Bruni S, Bruschi B, Carloni I, Coppa GV (2002) Kabuki syndrome and growth hormone deficiency: description of a case treated by long-term hormone replacement. Clin Dysmorphol 11(1):71–72
15. Allen RC, Zoghbi HY, Moseley AB, Rosenblatt HM, Belmont JW (1992) Methylation of HpaII and HhaI sites near the polymorphic CAG repeat in the human androgen-receptor gene correlates with X chromosome inactivation. Am J Hum Genet 51(6):1229–1239
16. Micale L, Augello B, Fusco C, Selicorni A, Loviglio MN, Silengo MC, Reymond A, Gumiero B, Zucchetti F, D'Addetta EV, Belligni E, Calcagnì A, Digilio MC, Dallapiccola B, Faravelli F, Forzano F, Accadia M, Bonfante A, Clementi M, Daolio C, Douzgou S, Ferrari P, Fischetto R, Garavelli L, Lapi E, Mattina T, Melis D, Patricelli MG, Priolo M, Prontera P, Renieri A, Mencarelli MA, Scarano G, della Monica M, Toschi B, Turolla L, Vancini A, Zatterale A, Gabrielli O, Zelante L, Merla G (2011) Mutation spectrum of MLL2 in a cohort of Kabuki syndrome patients. Orphanet J Rare Dis. 9(6):38–45
17. Hannibal MC, Buckingham KJ, Ng SB, Ming JE, Beck AE, McMillin MJ, Gildersleeve HI, Bigham AW, Tabor HK, Mefford HC, Cook J, Yoshiura K, Matsumoto T, Matsumoto N, Miyake N, Tonoki H, Naritomi K, Kaname T, Nagai T, Ohashi H, Kurosawa K, Hou JW, Ohta T, Liang D, Sudo A, Morris CA, Banka S, Black GC, Clayton-Smith J, Nickerson DA, Zackai EH, Shaikh TH, Donnai D, Niikawa N, Shendure J, Bamshad MJ (2011) Spectrum of MLL2 (ALR) mutations in 110 cases of Kabuki syndrome. Am J Med Genet A 155A(7):1511–1516
18. Paulussen AD, Stegmann AP, Blok MJ, Tserpelis D, Posma-Velter C, Detisch Y, Smeets EE, Wagemans A, Schrander JJ, van den Boogaard MJ, van der Smagt J, van Haeringen A, Stolte-Dijkstra I, Kerstjens-Frederikse WS, Mancini GM, Wessels MW, Hennekam RC, Vreeburg M, Geraedts J, de Ravel T, Fryns JP, Smeets HJ, Devriendt K, Schrander-Stumpel CT (2011) MLL2 mutation spectrum in 45 patients with Kabuki syndrome. Hum Mutat 32(2):2018–2025
19. Li Y, Bögershausen N, Alanay Y, Simsek Kiper PO, Plume N, Keupp K, Pohl E, Pawlik B, Rachwalski M, Milz E, Thoenes M, Albrecht B, Prott EC, Lehmkühler M, Demuth S, Utine GE, Boduroglu K, Frankenbusch K, Borck G, Gillessen-Kaesbach G, Yigit G, Wieczorek D, Wollnik B (2011) A mutation screen in patients with Kabuki syndrome. Hum Genet 136(6):715–724
20. Issaeva I, Zonis Y, Rozovskaia T, Orlovsky K, Croce CM, Nakamura T, Mazo A, Eisenbach L, Canaani E (2007) Knockdown of ALR (MLL2) reveals ALR target genes and leads to alterations in cell adhesion and growth. Mol Cell Biol 27(5):1889–1903

European Journal of Medical Genetics 56 (2013) 526–528

Contents lists available at ScienceDirect

European Journal of Medical Genetics

journal homepage: http://www.elsevier.com/locate/ejmg

Array report

# A 2.0 Mb microdeletion in proximal chromosome 14q12, involving regulatory elements of *FOXG1*, with the coding region of *FOXG1* being unaffected, results in severe developmental delay, microcephaly, and hypoplasia of the corpus callosum

Masaki Takagi [a,b], Goro Sasaki [c], Toshikatsu Mitsui [a], Misa Honda [c], Yoko Tanaka [c], Tomonobu Hasegawa [a,*]

[a] *Department of Pediatrics, Keio University School of Medicine, Tokyo, Japan*
[b] *Department of Endocrinology and Metabolism, Tokyo Metropolitan Children's Medical Center, Tokyo, Japan*
[c] *Department of Pediatrics, Tokyo Dental College Ichikawa General Hospital, Ichikawa, Japan*

ARTICLE INFO

*Article history:*
Received 30 August 2012
Accepted 30 May 2013
Available online 26 July 2013

*Keywords:*
FOXG1
PRKD1
Regulatory elements
14q12
Array CGH assay

ABSTRACT

We identified 2.0 Mb of a novel deletion on chromosome 14q12, involving 8 genes and putative regulatory elements of *FOXG1* by array CGH in a patient with severe growth and psychomotor retardation, hypotonia, microcephaly, dysmorphic face, and hypoplasia of the corpus callosum. Case of a submicroscopic 14q12 deletion, involving regulatory elements of *FOXG1*, with the coding region of *FOXG1* being unaffected, is extremely rare.

Using fibroblast cell line established from the patient, we showed that the expression level of *FOXG1* in our patient was decreased. Our finding provides additional evidence that not only over-dosage of FOXG1 as previously mentioned, under-dosage of FOXG1 is also associated with phenotype, overlapping between congenital variant of Rett syndrome with *FOXG1* mutations and 14q12 microdeletion, not including the coding region of *FOXG1*. Though the gene dosage of *FOXG1* appears to be critical for the normal development of brain, the complex mechanism of its regulation of gene expression remains to be elucidated.



## 1. Methods of detection

### 1.1. Array CGH analysis

After genetic counseling, we obtained written informed consent from the parents for molecular studies, which were approved from the Institutional Review Board of the Keio University School of Medicine. Genomic DNAs were extracted from peripheral blood of the patient and parents using standard techniques, subjected to array comparative genomic hybridization (aCGH) with the Agilent 4 × 180K SurePrint G3 Human CGH Microarray (catalog no. G4449A; Agilent Technologies, Santa Clara, CA).

### 1.2. Chromosomal anomaly

The array CGH assay for the patient revealed a heterozygous interstitial deletion, which was of estimated minimum extent 2.05 Mb, extending from bp 29,677,089 to bp 31,731,999 on chromosome 14q12 (NCBI Build 37/hg 19) (Fig. 1A). Maximum size was 2.14 Mb, from bp 29,615,149 to bp 31,755,257. The deletion included 8 genes (*PRKD1*, *G2E3*, *SCFD1*, *COCH*, *STRN3*, *MIR624*, *AP4S1*, and *HECTD1*).

### 1.3. Method of confirmation

FISH was performed on metaphase slides from peripheral blood lymphocytes using standard techniques. The deletion was confirmed using the RP11-369O9 clones (Fig. 1B). CGH analysis of the parents revealed that this deletion was *de novo* (data not shown).

* Corresponding author. Department of Pediatrics, Keio University School of Medicine, 35 Shinanomachi, Shinjuku-ku, Tokyo 160-8582, Japan. Tel.: +81 3 3353 1211.
*E-mail address:* thaseg@a6.keio.jp (T. Hasegawa).

1769-7212/$ – see front matter © 2013 Elsevier Masson SAS. All rights reserved.
http://dx.doi.org/10.1016/j.ejmg.2013.05.012

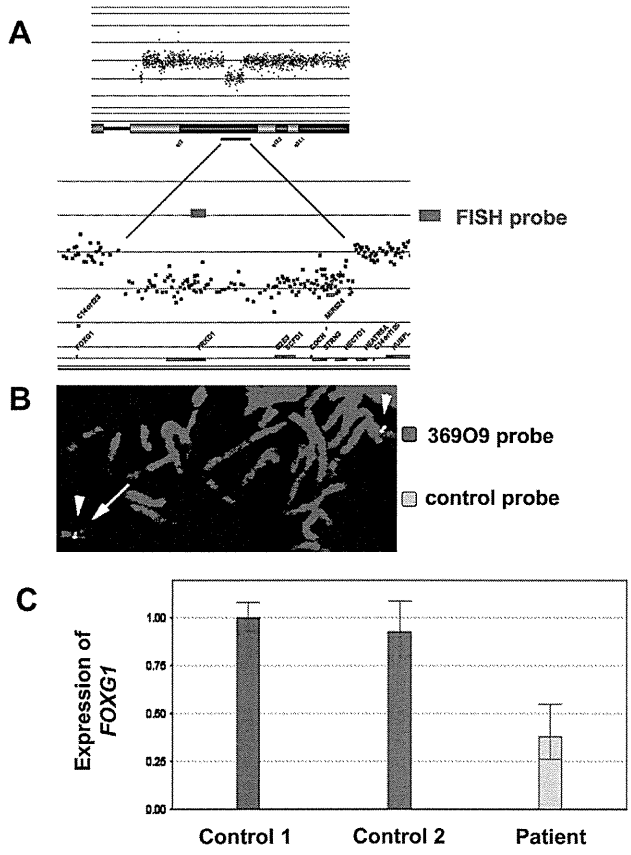


**Fig. 1.** Result of CGH array analysis, FISH validation, and quantification of the expression of *FOXG1*. A: Graphical representation of the results of the array CGH analysis [Agilent 4 × 180K SurePrint G3 Human CGH Microarray] shows a 2.0 Mb interstitial deletion of 14q12, including 8 genes. B: FISH analysis for validation of array CGH result. The patient under study shows a deletion of RP11-369O9 [red] located on 14q12 (arrow). C: Real-Time PCR revealed that the level of *FOXG1* transcripts of the patient was about 40% the control level.

### *1.4. Expression of FOXG1 in the patient with 14q12 microdeletion*

Total RNA was extracted from lymphoblastoid cell line established from the patient and cDNA synthesis was performed with the SuperScript III reverse transcriptase kit (Invitrogen, Carlsbad, CA) with oligoDT primers. Real-time quantitative PCR was performed on the ABI PRISM 7500 Fast Real-Time PCR System (Applied Biosystems, Foster City, CA). For PCR reaction, we used SYBR Premix Ex Taq II (Takara, Otsu, Japan). The relative quantification was performed with the 2-DDCt method relative to a constitutively expressed gene (*GAPDH*). All reactions were carried out in triplicate and expression levels were determined in 3 independent experiments. Real-Time PCR revealed that the level of *FOXG1* transcripts of the patient was about 40% the control level (Fig. 1C).

## 2. Clinical description

The patient, an 11-year-old Japanese boy, was the first child of non-consanguineous healthy parents. He was born at term after uneventful pregnancy and delivery, and his birth weight, length, and OFC were 2706 g (10–25th percentile), 49.0 cm (25–50th percentile), and 31.5 cm (3rd–10th percentile), respectively. At the age of 6 month, he was referred to our hospital for evaluation of developmental delay and dysmorphic features. He exhibited hypotonia with incomplete head control, microcephaly (OFC, 40.1 cm, below 3rd percentile), and facial anomaly including hypertelorism, epicanthal folds, depressed and broad nasal bridge, and short neck (Fig. 2A). Cortical atrophy of parietooccipital lobes, delayed myelination, and hypoplasia of the corpus callosum (HCC) were demonstrated on brain MRI (Fig. 2B), while no malformation was displayed in heart and kidney ultrasonography, and no overt hearing loss was evidenced in auditory brainstem response. He also presented frequent generalized seizures, which were well controlled with phenobarbital and sodium valproate. Growth and psychomotor development were severely retarded. At 11 years of age, his weight, length, and OFC were 15.5 kg (below 3 percentile), 107.0 cm (below 3 percentile), and 47.4 cm (below 3rd percentile), respectively. No apparent skeletal deformity was documented on X-ray, and plasma concentrations of thyroxine and insulin-like growth factor-1 were within normal ranges. Due to severe psychomotor retardation, he remains wheelchair-bound and nonverbal.

## 3. Discussion

We identified 2.0 Mb of a novel deletion on chromosome 14q12, involving 8 genes and putative regulatory elements of *FOXG1* by using array CGH in a patient with severe growth and psychomotor

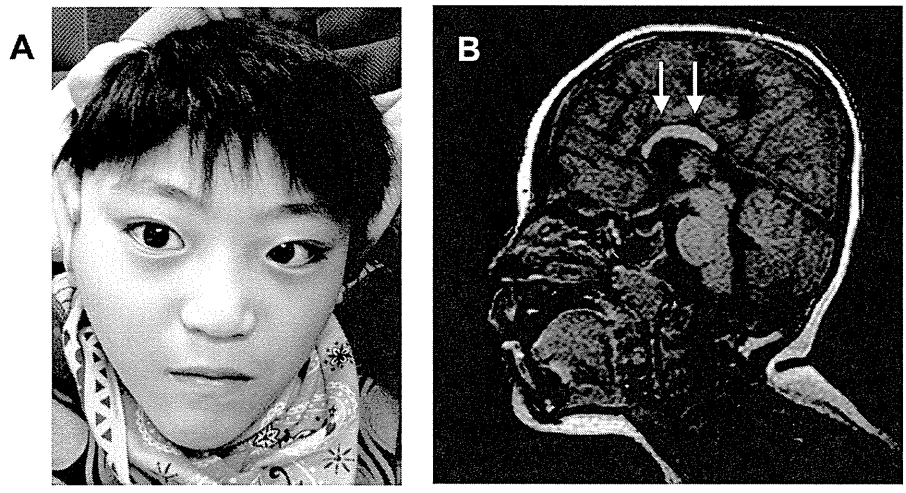


**Fig. 2.** Features of the patient with deletion on chromosome 14q12. A: Photographs of the patient at 10 years of age. Facial features demonstrated ocular hypertelorism, epicanthal folds, depressed and broad nasal bridge, and short neck. B: Brain imaging in the patient at the age of 5 years. Arrow indicates hypoplasia of the corpus callosum.